38. ORGANIC MATTER IN PERU UPWELLING SEDIMENTS—ANALYSIS BY PYROLYSIS, PYROLYSIS-GAS CHROMATOGRAPHY, AND PYROLYSIS-GAS CHROMATOGRAPHY MASS SPECTROMETRY[1]

Jean K. Whelan,[2] Zoltan Kanyo,[2] Martha Tarafa,[2] and Mark A. McCaffrey[2]

ABSTRACT

Significant variations in the nature and content of total carbon and total organic carbon (TOC) in closely spaced near-surface samples from Sites 681, 686, and 683 are accompanied by changes in pyrolysis parameters. All TOC, pyrolyzable carbon values (P_2), and hydrogen index (HI) values (e.g., P_2 normalized to TOC) were found to be significantly higher in Hole 681A sediments, compared with those from Sites 686 and 683. Samples from Hole 681A contained almost no carbonate. T_{max} values (e.g., maximum temperature of P_2 evolution) generally were highest for Site 683 sediments, possibly indicating a greater influx of more reworked or terrigenous organic matter at this site, which is situated on the slope, at the edge or outside of today's upwelling area. TOC and pyrolysis (P_2) values correlated in closely spaced near-surface samples from Hole 681A (correlation coefficient, $r = 0.78$), with correlation decreasing for Holes 686A ($r = 0.5$) and 683A ($r = 0.22$). On the basis of comparison with data from surface cores obtained by Woods Hole Oceanographic Institution, we postulate that the lack of correlation of P_2 and organic carbon values in several Site 683 intervals may indicate that these intervals contain more terrigenous or more reworked marine organic carbon. PI values showed poor correlation with TOC values at all three sites. Variations in PI values, which generally fall in the immature range of 0.04 to 0.08, are thought to show the relative amounts of *in-situ* marine biogenic (rather than petrogenic) influence.

Pyrolysis-gas chromatography mass spectrometry (PY-GCMS) patterns for a few ODP samples were compared with those for an extensive set of Peru surface samples (from three Woods Hole Oceanographic Institution cruises to the same area). The results suggest that the three ODP sections examined here were most strongly influenced by organic matter derived from marine upwelling (rather than terrigenous) influx, even at Site 683. Minimal influence by terrigenous influx is consistent with the desert nature of the Peru coast, which is only sparsely vegetated. Pyrolysis-GCMS data also suggest that *Thioploca* bacterial mats, diagnostic of suboxic bottom waters in this region, may be a source of the sporadic thiophene pyrolysis products observed in some Peru sediments.

INTRODUCTION

This study examines the diagnostic pyrolysis, pyrolysis-gas chromatography (PY-GC) and PY-GCMS signals characteristic of the various depositional environments within the Peru upwelling region. These techniques now are extensively used for studies of petroleum source rocks in conjunction with oil and gas exploration (Espitalié et al., 1984; Larter, 1984; Peters, 1986; Tissot, 1984; Horsfield, 1984; Katz, 1983; Orr, 1981; Philp, 1985). Some problems have arisen from catalytic effects of the mineral matrix when attempting to apply these methods to some types of samples, such as those containing the clay mineral smectite or which are organic lean (less than 0.5% TOC, Katz, 1983; Larter, 1984; Orr, 1981). Most scientists agree that the problem is minimal in organic-rich sediments, such as those analyzed and described here. Arnosti and Müller (1987) reached similar conclusions using the same apparatus as that used here.

Effects of depositional environment on pyrolysis parameters of sedimentary organic matter usually have not been considered in past work because of the lack of background data from well-defined contemporary analogs of ancient source rocks. This is particularly true for various types of organic-rich marine sediments that constitute excellent oil sources in several parts of the world (such as the Monterey

Formation of the California Borderland). Examination of pyrolysis character in the context of excellent sets of ancillary geological and geochemical data obtained for Leg 112 sediments offers us an excellent opportunity to relate pyrolysis data to various depositional processes occurring within the Peru upwelling region. In addition, Woods Hole scientists have conducted three cruises in the same general area (Farrington et al., 1988; Henrichs and Farrington, 1984; Henrichs et al., 1984;, McCaffrey, et al, 1989; Volkman et al., 1983, 1987; Whelan and Hunt, 1983), so that organic geochemical data from surface sediments, sediment traps, and the water column also are available for comparison in this and future studies.

Some excellent PY-GCMS studies of contemporary marine environments have been conducted, principally on inshore and coastal environments, with somewhat different methods than those used here (van de Meent et al., 1980; Sigleo et al., 1982). We have in the past performed PY-GCMS studies on water-column particulates and sediments from a municipal harbor (Whelan et al., 1980, 1983); a coastal marsh (Whelan et al., 1986a), as well as immature DSDP deep water marine sediments (offshore New Jersey, Leg 95, Tarafa et al., 1987; Sites 504 and 505, Whelan and Hunt, 1982; southwest Africa, Leg 75, Jasper et al., 1984; and Japan Trench, Leg 56, fecal pellets, Thompson and Whelan, 1980) and sediments dominated by terrigenous organic matter from the Gulf of Mexico (Whelan and Tarafa, 1986; Whelan, 1986). Leg 112 sediments offer scientists an excellent opportunity to apply these same techniques to more organic-rich marine sediments in order to better define pyrolysis organic geochemical signals diagnostic

of upwelling and productivity. In addition, these data can be used with other organic geochemical and geological data to interpret better the much less detailed Rock-Eval data, which because of the routine shipboard measurements aboard the *JOIDES Resolution*, are now available from a wide variety of deep-ocean sediments, including those from Peru.

METHODS

Total carbon was measured for samples weighed onto 0- to 7-μm glass fiber filters, each of which were combusted at 900°C. The evolved CO_2 was measured in a Coulometric CO_2 Coulometer (Curry and Miller, in press). Analytical precision for this measurement is ±0.05% TOC. TOC was determined for a weighed sample on the glass fiber filter paper that had been treated for at least three days with vapor from concentrated hydrochloric acid in a desiccator, followed by treatment with the vapor from concentrated ammonium hydroxide in a second desiccator for at least 15 min (Jasper et al., 1984). The samples on the filter paper were then dried at 60°C, combusted, and the evolved CO_2 measured coulometrically, as described above.

PY-GC data were obtained by methods described in detail elsewhere (Whelan et al., 1983, 1986a; Tarafa et al., 1987). Briefly, the procedure was as follows: 50 to 100 mg of wet sediment was ground with a mortar and pestle and placed in a quartz tube between two pieces of quartz wool. The tube was placed in a desorption probe in the cooled interface of a Chemical Data Systems (CDS) Model 820 Geological Reaction System and heated at 30°C/min from 200° to 600°C. Organic compounds desorbed during the heating process were swept out of the system in a helium stream. The stream was split three ways, with part going directly to a flame ionization detector (FID), a second part being trapped for GC analysis and a third part being trapped for GCMS analysis.

During the heating process, the compounds evolved as two peaks—the lower temperature peak (P_1), evolving at 200° to 250°C, represented volatilization of free or sorbed organic compounds present in the sediment; the higher temperature peak (P_2), evolving at 400° to 500°C, consisted primarily of compounds cracked (thermal cleavage) from the sediment kerogen or protokerogen (high molecular-weight organic) matrix. P_2 also can include higher molecular-weight components of heavy bitumen, which only volatilize at high temperature. (Note: the term "organic matrix" used here has an operational definition that includes all organic matter not volatilized from the sample during the collection of P_1 values. This may include nonvolatile low-molecular-weight compounds, such as fatty acids, amino acids, and sugars; biogenic polymers, such as proteins; and geopolymers, such as humic and fulvic acids and kerogen.) The temperature of the maximum height of the P_2 peak, called T_{max}, was measured using a thermocouple placed next to the sediment sample. Note that this procedure gives those temperatures to which the sample was actually subjected; these are consistently about 60°C higher than Rock-Eval T_{max} values. This consistently "low" offset of nominal Rock Eval T_{max} values was discussed in detail by Espitalié et al. (1984), who pointed out that for most applications, only internally consistent T_{max} values are required, as produced by the Rock Eval (rather than accurate values, which are reported here).

Note that the designations "P_1" and "P_2" are used here to distinguish our results from those obtained from the more widely used Rock-Eval pyrolysis apparatus, where the designations "S_1" and "S_2" are used. This distinction is necessary because the two pyrolysis instruments differ in design and give somewhat different values, such as those for T_{max}, discussed above. In addition, the P_1 and P_2 peaks are much better separated with the CDS than with the Rock-Eval instrument, which can affect significantly the quantitation of the two peaks.

The second part of the helium stream from the CDS pyrolyzer used here was passed through an eight-port valve and trapped at 25°C in two traps (one for P_1 and one for P_2) packed with a porous polymer, Tenax (60 to 80 mesh, Applied Science Inc., State College, PA). By a series of heating and cooling cycles, trapped compounds were desorbed from the Tenax and analyzed by capillary GC to give a chromatogram characteristic of the C_6 to C_{28} volatile organic compound composition of the trapped mixture. A 0.0254-cm inner diameter × 25 m bonded-phase silica (SE54) capillary column was used to obtain GC traces (conditions: initial backflush desorption time from the Tenax trap: 15 min at 280°C to a second identical Tenax trap; 5 min backflush desorption onto the front of the capillary column held at 25°C; then programming of the GC oven from 25° to 300°C at 4°C/min.)

Other scientists have had problems with the CDS apparatus and the Tenax trapping procedure described above. We also experienced difficulties whenever the instrument was shut down for an extended period of time or when the Tenax traps had been exposed to air, particularly at high temperatures. We also determined that Tenax has a substantial background bleed when first obtained and can have severe memory effects when overheated, particularly in the presence of air. Therefore, the Tenax in our system (1) was never heated to temperatures of more than 280°C, (2) was never exposed to air, and (3) the traps on the CDS instrument were never repacked unless they had been accidently overheated. We also determined that periodic loses of the higher molecular weight fractions on the gas chromatogram (above about C_{18}), which often occurred after the instrument had been shut down, could be eliminated by running an organic-rich sample, such as a Messel or Green River shale sample, through the system. Note also that the CDS system was not designed to analyze quantitatively the higher molecular-weight compounds (above C_{30}). Much better instruments and technologies are currently available for this purpose (such as the commercially available all-quartz Ruska system).

GC compositions obtained for both P_1 and P_2 peaks are highly reproducible; precisions of ±5% are routinely obtained on resolved individual P_2 capillary GC peaks for n-alkanes and aromatic hydrocarbons for both modern and ancient sediments. For less well-resolved and more labile peaks, coefficients of variation are higher: average of 8% for C_9 and above (1 σ range 3%–12%) and an average of 24% for C_6 through C_8 (1 σ range 5%–32%) in the concentration range of 10 to 500 ng of compound per gram dry weight of sediment. The higher variability of the C_6 through C_8 compounds result from both the poorer resolution of these early eluting peaks and the greater losses of the more volatile compounds that occur during sample preparation. Whelan et al. (1983) noted that these analytical precisions compared favorably, and were often superior, to those reported for other methods of analyzing complex organic mixtures in natural systems.

The third stream of the pyrolyzer (for GCMS analysis) was directed toward a ⅛ in. (3.2 mm) outer diameter × 3 in. (7.6 cm) stainless steel tube packed with 60 to 80 mesh Tenax, previously conditioned overnight in a helium stream at 280°C and stored under nitrogen until used (generally as soon as possible after conditioning). Mass spectral analyses were performed by desorbing the Tenax traps into a GCMS (Carlo Erba model 4160 GC equipped with a cryogenic oven attachment connected to a Finnigan 4500 quadrupole mass spectrometer). The traps were desorbed in a helium stream through a heated desorption module that was attached to the
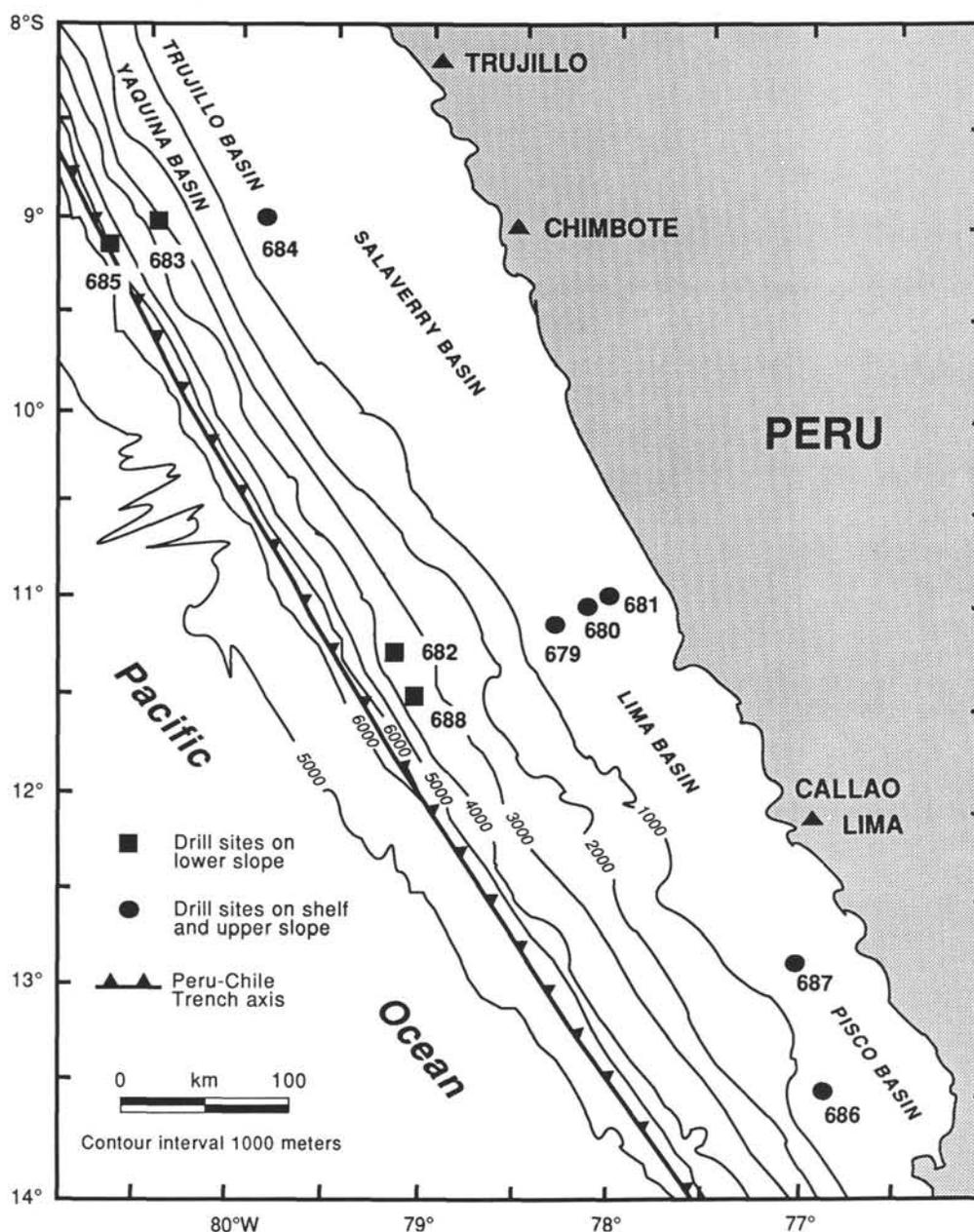
Figure 1. Map showing site locations, Leg 112, Peru margin and shelf.

GC injection port. The GC oven was cooled to −20°C, while the desorption heater was heated to 280°C and then maintained at that temperature for 15 min. The GC oven was then ramped to 40°C, and the bonded phase capillary column, identical to that used for the capillary GC analysis described above, was programmed from 40° to 280°C at 4°C/min. Mass spectra were acquired using electron impact ionization at 70 eV, scanning from 40 to 350 amu at 1-s intervals. The GCMS system was connected to a Finnigan INCOS 2300 Data System that contained the NBS/EPS/NIH reference library of 31,000 spectra. Compounds were identified tentatively using the forward search algorithm included with the INCOS system. Confirmation of identification was then conducted by comparison with retention times and mass spectra obtained for standards run in our own laboratory. The more exotic structures from pyrolysis of lignins and carbohydrates were

confirmed by having our samples run in the laboratory of J. Boon, FOM Institute AMOLF, Kruislaan, The Netherlands.

RESULTS AND DISCUSSION

Sections Examined

The locations of the ODP and Woods Hole cores examined here are shown in Figures 1 and 2, respectively. Visual descriptions and depths of the ODP samples are shown in Table 1. A summary of pyrolysis data for Peru ODP and Woods Hole samples and a comparison of these samples to DSDP data from other areas is shown in Table 2. The intervals examined were obtained from shallow sections (<40 m below the seafloor, mbsf) from three holes (Fig. 1). Hole 681B is the shallowest and most landward of the sites drilled during Leg 112. The location of the site at 11°S and a water depth of 150.5
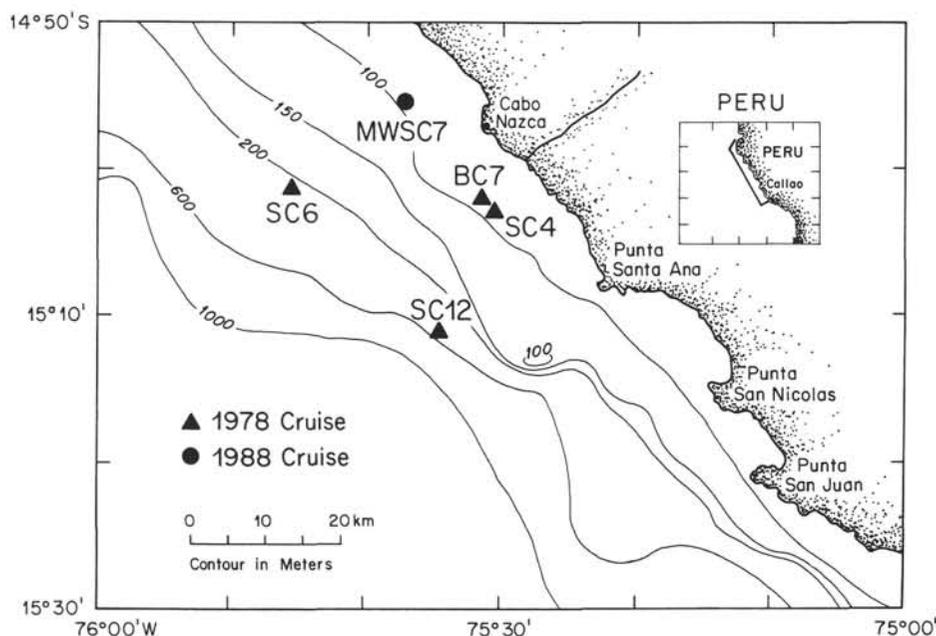
Figure 2. Map showing locations, Woods Hole surface cores. Map shows site locations of the *Knorr* cruise in 1978 and of the *Moana Wave* cruise in 1988.

m coincides with the top of the oxygen-minimum zone (Suess et al., this volume). The approximate relationship between the oxygen-minimum zone and water depth can be estimated from Figure 3 (Henrichs et al., 1984; Farrington, unpubl. data), which was made as part of the Woods Hole 1978 cruise at 15°S; however, one should keep in mind that the exact position of the oxygen-minimum zone can vary both temporally and spatially. Hole 683A is located farther north at 9°S in deeper water (about 3100 m), within the northern fringe of the upwelling region, but outside the oxygen-minimum zone. Hole 686A is located farther south, also within today's upwelling area at a water depth of 457 m, a depth corresponding to the outer edge of the oxygen-minimum zone. Hole 686A lies within the West Pisco Basin and is shielded by the East Pisco Basin from terrigenous influx, if terrigenous influx occurs directly across the shelf.

Pyrograms

Pyrograms were used extensively in this study because these can be obtained rapidly, compared with data obtained by other organic geochemical techniques (such as solvent extraction and PY-GCMS). Our strategy was to use the pyrograms as a screening technique for selecting samples for more labor-intensive types of organic geochemical analyses. Total carbon, organic carbon, and pyrogram data for four closely spaced surface intervals of the Peru ODP sections examined here are shown in Figures 4 through 11 and in Tables 2 and 3. The parameters shown include profiles of total pyrolyzable carbon (P_2), total sorbed (inherited, generated, and migrated) organics (P_1), the HI (P_2/TOC in milligrams of P_2 hydrocarbons/g TOC), the PI [$P_1/(P_1 + P_2)$, which is the ratio of sorbed to total sorbed and pyrolyzable organic matter], and T_{max}.

A summary of the behavior of each of these parameters for the samples examined is presented next.

Total Pyrolyzable Carbon (P_2)

P_2 (called S_2 in Rock-Eval pyrolysis analysis; see "Methods" section, this chapter) is used extensively in petroleum exploration to indicate oil-generating potential in a particular

section. Because the FID detector used to measure the pyrograms responds to combustible material, which in these samples consists primarily of reduced carbon, this signal also gives a measure of how much hydrogen is contained in the organic matter, expressed in petroleum source-rock analysis as the "hydrogen index" (HI), which is milligrams of P_2 (predominantly hydrocarbon) per gram of TOC. In our laboratory, the HI was used not only to obtain information concerning changes in depositional environment, but also to obtain the degree of reworking prior to and just after deposition; these processes affect the HI because metabolism of organic matter by organisms also reduces the ratio of hydrogen to carbon in sediment organic matter (e.g., Durand and Monin, 1980; Whelan and Tarafa, 1986; Tarafa et al., 1987). Thus, sediment organic carbon and P_2 are often found to be directly proportional (e.g., Jasper et al., 1984; Whelan and Hunt, 1982). The slope of the line is proportional to the HI, with higher HIs indicating better petroleum source rocks. However, because TOC can also include a high proportion of reworked or thermally degraded (i.e., hydrogen-poor) carbon, cases where this proportionality does not occur can provide information about changes in depositional processes, including the degree of biodegradation and the proportions of organic matter derived from different biological sources.

P_2 data for the four sections analyzed here are shown in Figures 4 through 12 and Tables 2 and 3. For comparison, similar data for Woods Hole surface cores (where considerably more information is available about exact depositional processes, Henrichs and Farrington, 1984; Farrington et al., 1988) also are summarized in Table 2. These results suggest the following (which will be investigated further in future work):

1. The highest P_2 values occur in both of the sequences from Hole 681B and are comparable to results from Woods Hole surface core MWSC7 (Table 2). These values are generally lower (by about two to six times) than those for Woods Hole surface Cores SC6 and SC12, which were recovered from the center of the 1978 upwelling zone. High P_2 values are typical of sediments that have not undergone a high degree of reworking (i.e., bacterial degradation) prior to deposition

(e.g., Tarafa et al., 1987; Whelan and Tarafa, 1986). These results suggest that the laminated sections from both the 0.4 to 3 m and the 6.19 to 6.78 m sections of the Hole 681B cores were deposited under conditions similar to those of Core MWSC7, i.e., shallow water, strong upwelling, and probably, although not necessarily, within the oxygen-minimum zone.

2. Lower P_2 values in the 1.04 to 1.09 m sections of Hole 683A and the 3.62 to 3.74 m sections of Hole 686A are comparable to those of Woods Hole surface Cores SC4 and BC7, which were recovered from the upwelling area, but on the edge of the oxygen-minimum zone (Farrington et al., 1988). These results are consistent with sections from both Holes 683A and 686A being deposited in the upwelling zone, but perhaps not in the oxygen-minimum zone. However, the low P_2 values for Hole 683A, comparable to the range observed in Core SC4 surface sediments, probably also reflect the deposition of the Hole 683A sediments in deeper water, where organic matter has more opportunity for reworking before deposition.

Total Sorbed (Inherited, Generated, or Migrated) Organics (P_1) and the Production Index, ($P_1/P_1 + P_2$)

Profiles for P_1 for these three sections are shown in Figures 5, 6B, 8, and 11. In petroleum exploration, the production index (PI) gives a relative measure of bitumen naturally present in (or which has migrated into) a particular section. In modern sediments, which have not experienced catagenetic petroleum hydrocarbon generation, this parameter is typically small, i.e., less than 10% of P_2 values. The small P_1 values that are detected in these sediments are typical of biogenic (rather than petrogenic) material (e.g., Whelan and Tarafa, 1986; Tarafa et al., 1987; Jasper et al., 1984).

PI values are usually calculated for petroleum source rocks. In immature sediments, where P_1 is coming directly from residual biogenic material, PI values are generally less than 0.1 and are often less than 0.05. In deeper, thermally mature sediments undergoing catagenetic hydrocarbon generation, PI values are typically 0.1 to 0.5, while intervals containing migrated petroleum exhibit high values (typically greater than 0.8 and often approaching 1, Espitalié et al., 1984).

The intervals examined here exhibit the following trends in P_1 and PI:

1. The concentrations of P_1 are generally higher for the 0.4 to 2.2 m section of Hole 681B than for the 6.25 to 6.8 m section (Table 2; also, compare Figure 5 with Figure 6B). The P_1 levels for the 6.25 to 6.8 m section of Hole 681B are in the same range as values for the 2.2 to 2.8 m section (500 to 600 $\mu g/g$, Fig. 5). These are in about the same range as values obtained for the Woods Hole surface sediments from shelf Core MWSC7 (Table 2). The 2.62 to 2.79 m section from Hole 683A exhibits average P_1 values in about the same range, but with much more scatter and possibly a periodic oscillation (Fig. 11). The 19.3 to 19.6 m and the 20.1 to 20.4 m sections of Hole 686A show some of the consistently lowest P_1 levels measured for these sample sets (less than 300 $\mu g/g$ and averaging about 150 $\mu g/g$, Fig. 8). These values are comparable with levels detected for the leanest of the Woods Hole surface cores, SC4 and BC7 (Table 1), both of which were recovered from shallow water on the continental shelf at the edge or outside of the present-day upwelling zone (Fig 3).

2. P_1, P_2, and PI values vary less smoothly with depth for the Hole 681B 0.6 to 1.8 m section (Fig. 5) in comparison with the deeper 6.25 to 6.8 m section (Fig. 6). However, variations in both of the Hole 681B P_1 profiles, as well as in the 19.8 to 20.4 m section of Hole 686A (Fig. 8), are fairly smooth

when compared to the fairly strong (cyclic?) variation apparent in the 2.6 to 2.8 m section of Hole 683A (Fig. 10) and the 19.35 to 20 m section of Hole 686B (Fig. 8). The depth scale for one of the apparent cycles for P_1, P_2, and PI for the 2.6 to 2.8 m section of Hole 683A is about 5 cm (Figs. 10 and 11). Assuming an overall deposition rate of about 100 m/m.y. (Suess, von Huene, et al., 1988), 5 cm should correspond to a time interval of about 500 yr for one these "pyrolysis" cycles. Average water contents and porosity show considerable scatter, but remain approximately constant over the top 80 m of this site (Suess, von Huene, et al., 1988); compaction effects, therefore, were not considered. Note that the P_1 and P_2 cyclicity may continue into deeper sections, but would not have been observed because the samples analyzed were not as closely spaced. In the 19.35 to 19.8 m section of Hole 686B, similar P_1 variations occur over about the same distances (Fig. 8). No apparent visual change occurs between the high and low P_1 and P_2 intervals within the 2.6 to 2.79 m section of Hole 683A, where all the sediments appeared to be homogeneous olive green and somewhat bioturbated (Table 1). However, within the 19.35 to 19.8 section of Hole 686A, there are variations of laminated, with more homogeneous (and in some cases bioturbated) sediment intervals. This interbedding occurs on about the same distance scale as the P_1-P_2-PI cycles (Table 1). In some (but not all) cases, the more laminated sections exhibit higher values of P_1 and P_2.

3. P_1 values are generally low and PI values are less than 0.1 (and often less than 0.06) in all of the sections analyzed, as expected for thermally immature surface sediments. PI values obtained for the ODP Peru sediments using the Rock-Eval instrument on board the *JOIDES Resolution* are considerably higher, generally in the range of 0.1 or more. These shipboard Rock-Eval values were repeated by analyzing the same samples with a different Rock Eval instrument on shore. We are at a loss to explain the high S_1 and PI values obtained using Rock-Eval instruments (Table 3). A low S_2 value of 6600 $\mu g/g$, in comparison to the P_2 value, also occurs in the 0.4 to 3 m interval of Hole 681B. This comparison shows that one must take care when interpreting shipboard Rock-Eval data. PI values consistently greater than 0.1 are generally interpreted in the petroleum industry as being diagnostic of sediments entering the petroleum catagenetic zone (e.g., Espitalié, 1984; Peters, 1986; Horsfield, 1984; Larter, 1984). However, that interpretation is not supported by other geological, geochemical, and geophysical data for the Leg 112 sediments.

4. In some sections, P_1 appears to track P_2, such as in the 1.8 to 2.8 m section of Hole 681B (Fig. 5) and the 2.6 to 3.05 m section of Hole 683A (Figs. 10 and 11). However, plots of P_1 vs. P_2 for each hole exhibit only a weak correlation for the two parameters ($r = 0.11$ to 0.5, Table 2). In most previous research, scientists, including those in our laboratory, have assumed that P_1 in recent sediments was too small to be interesting. Because this is one of the first sets of samples where we have obtained detailed profiles for both P_1 and P_2 in surface sediments, we are not certain how to interpret correlations (or lack thereof) of P_1 with P_2. A strong correlation of P_1 with P_2 was observed for the Peru surface sediments obtained during Woods Hole cruises, as shown in Figure 12 and Table 1 for Soutar Core MWSC7 ($r = 0.87$). A possible reason for this correlation, which should be tested in future research, would be that both the P_1 and P_2 values are derived predominantly from fresh, marine biological material (either volatilized or thermally decomposed) produced within the upwelling regime. Such a correlation would disappear as a result of any process that preferentially degrades either P_1 or P_2 (such as biodegradation) or that brings organic material from a different source into the system. For example, an

Table 1. Visual core descriptions of samples analyzed.

Sample	Depth (m)	Description	Description (general)
Hole 681B			
12-681B-1H, 1–47	0.47	Mottled	75% clay; 25% silt 25% diatoms; sponge spicules; CH$_4$ low throughout
1H-1, 57	0.57	"	
1H-1, 67	0.67	Homogeneous—dark	
1H-1, 77	0.77	"	
1H-1, 87	0.87	"	
1H-1, 97	0.97	"	
1H-1, 107	1.07	"	
1H-1, 117	1.17	"	
1H-1, 127	1.27	"	
1H-1, 137	1.37	Laminated—lighter bands	Diatoms 10%; silt 15%
1H-1, 147	1.47		
1H-2, 7	1.57	Verticle streaks	
1H-2, 17	1.67	"	
1H-2, 27	1.77	"	
1H-2, 37	1.87	Verticle streaks to mottled	
1H-2, 47	1.97	Dark—homogeneous	
1H-2, 57	2.07	"	
1H-2, 67	2.17	"	
1H-2, 77	2.27	"	
1H-2, 87	2.37	"	
1H-2, 97	2.47	"	
1H-2, 107	2.57	"	
1H-2, 117	2.67	Dark—homogeneous (just above lighter zone)	Shipboard data: TC = 2.35%; TOC =
1H-2, 127	2.77	Dark—homogeneous (above light zone)	2.35%; HI = 352; OI = 129 (mixed Type
1H-2, 137	2.87	Dark—homogeneous	II/III)
1H-2, 147	2.97	"	
2H-1, 29	6.19	Drilling disturb.? Verticle struc?	40% silt; trace diatoms
2H-1, 31	6.21		
2H-1, 34–35	6.24	Gas cracks	
2H-1, 38	6.28	Silty—unlaminated	40% silt
2H-1, 41	6.31	"	
2H-1, 44	6.34	"	
2H-1, 46	6.36	"	
2H-1, 48	6.38	"	
2H-1, 51	6.41	"	
2H-1, 52	6.42	"	
2H-1, 54	6.44	Silty—lighter streaks	
2H-1, 57	6.47	Silty—homogeneous—gas cracks?	
2H-1, 60	6.5	"	
2H-1, 62	6.52	"	
2H-1, 65	6.55	Silty—homogeneous—some light laminiae	
2H-1, 68	6.58	Silty—homogeneous—laminae more pronounced	
2H-1, 70	6.6	"	
2H-1, 72	6.62	"	
2H-1, 74	6.64	Siltier	
2H-1, 77	6.67	"	
2H-1, 82	6.72	Siltier—vert. cracks (from drill?)	"1–92 20% to 25% diatoms
2H-1, 86	6.76	"	
2H-1, 88	6.78	Lighter laminae—similar to 1–92	10% calcite; 20% silt
683A-2H-1, 43–44	2.63	Bioturbated throughout; olive green	"3–4% TOC; HI ≈ 250; OI ≈ 57
2H-1, 44–45	2.64		
2H-1, 45–46	2.65		
2H-1, 46–47	2.66		
2H-1, 47–48	2.67		
2H-1, 48–49	2.68		
2H-1, 49–50	2.69		
2H-1, 50–51	2.7		
2H-1, 51–52	2.71	"20:40:40 sand:silt:clay; 20% feldspar; 5% pyrite; " 10% forams; 35% diatoms; crack	
2H-1, 52–53	2.72		
2H-1, 53–54	2.73		
2H-1, 54–55	2.74	Some lamination	
2H-1, 55–56	2.75	"	
2H-1, 57–58			
2H-1, 57–58	2.77	Lamination + bioturbation	
2H-1, 63–64	2.83	"	
2H-1-65–66	2.85	"	
2H-1, 67–68	2.87	"	

Table 1 (continued).

Sample	Depth (m)	Description	Description (general)
2H-1, 69–70	2.89	"	
2H-1, 70–71	2.9	"	
2H-1, 75–76	2.95	"	
2H-1, 80–81	3	"	
2H-1, 85–86	3.05	(Section 102: more sand than 1H-52)	
686A-3H-4, 25–26	19.35	Homogeneous green—some laminae	HI ≈ 250; OI ≈ 125
3H-4, 26–27	19.36	"	(shipboard data)
3H-4, 27–28	19.37	"	
3H-4, 28–29	19.38	"	
3H-4, 29–30	19.39	"	
3H-4, 30			
3H-4, 31			
3H-4, 31–32	19.41	"	
3H-4, 32–33	19.42	"	
3H-4, 33–34	19.43	Homogeneous green; laminae more pronounced	
3H-4, 34–35	19.44	Bioturbated	
3H-4, 35–36	19.45	"	
3H-4, 36–37	19.46	Laminae—lighter (+bioturbation?)	
3H-4, 37–38	19.47	"	
3H-4, 38–39	19.48	Laminae + bioturbation	
3H-4, 39–40	19.49	"	
3H-4, 41–42	19.51	Laminae + more homogeneous	
3H-4, 43–44	19.53	"	
3H-4, 45–46	19.55	"	
3H-4, 47–48	19.57	Laminated—no bioturbation	
3H-4, 49–50	19.59	More homogeneous	
3H-4, 52–53	19.62	Laminated, no bioturbation	
3H-4, 55–56	19.65	More homogeneous	
3H-4, 60–61	19.7	Laminated—just above phosphorite	
3H-4, 65–66	19.75	Darker—laminated	
3H-4, 70–71	19.8	More homogeneous—bioturbated	
3H-4, 75–76	19.85	Laminated	
3H-4, 80–81	19.9	"	
3H-4, 85–86	19.95	Laminated—darker	
3H-4, 90–91	20	Laminated—lighter	
3H-4, 95–96	20.05	Laminae, lighter, bioturbation(?)	
3H-4, 100–101	20.1	Laminae—darker band	
3H-4, 105–106	20.15	Laminated—bioturbated—siltier	
3H-4, 110–111	20.2	Weaker laminae—siltier	
3H-4, 115–116	20.25	Lighter—weaker laminae	
3H-4, 120–121	20.3	Strong laminiae	
3H-4, 125–126	20.35	Strong laminiae—darker	
686B-1H-1, 42–47	0.42	Laminae, phosphorite	Organic C = 4–5%
1H-1, 78–82	0.78	Bioturbation	
1H-3, 111–115	4.11	Laminated	
1H-5, 115–120	7.15	Bioturbated (phosphorite?)	
3H-2, 45–49	19.95	Laminated (no bioturbation)	
9H-5, 58–62	81.58	"	

influx of terrigenous material might elevate P_2, but not P_1, if the sorbed fraction had been preferentially removed either by water washing or biodegradation during transport.

T_{max} (Temperature at Which Maximum Rate of P_2 Evolution or Pyrolysis Breakdown of Sediment Organic Matter Occurs)

The temperature of maximum P_2 yield, or T_{max}, is widely used in petroleum source-rock analysis as a maturation (time-temperature) indicator. The P_2 peak consists predominantly of products from a variety of reactions in which organic molecules are cracked from the sediment organic matter (predominantly kerogen) matrix. There also may be some contribution to P_2 from high molecular-weight volatilized material during this pyrolysis heating. Because each of these reactions has slightly different energy requirements, total P_2 evolution occurs as a broad Gaussian curve, with a characteristic maximum temperature, T_{max}. As a particular kerogen undergoes thermal reaction, the weakest bonds break first at the lowest temperatures; more energy is required to break the remaining kerogen bonds, and T_{max}

shifts to higher temperature as the sample undergoes increasing thermal maturation. This process and the relationship of T_{max} to thermal maturation have been discussed in detail for petroleum source rocks in recent reviews (Espitaliè et al., 1984; Ungerer et al., 1986).

The ODP sample set examined here shows low T_{max} values typical of immature surface samples (T_{max} = 446° to 472°C, Table 1). For comparison, some typical T_{max} values for other immature surface samples are also shown in Table 2. Thus, the Woods Hole Peru surface samples show T_{max} values in the range of 446 to 465°C, while the more terrigenous Mississippi Delta samples show slightly higher T_{max} values, ranging from 462° to 479°C (Whelan and Tarafa, 1986). Because T_{max} can be measured with a precision of about ±3°C, a small and measurable difference apparently occurs in T_{max} between the two types of samples. The reason for these differences between the marine upwelling sediments and the more terrigenous Mississippi Fan sediments may be either or both of the following: (1) the Mississippi Fan organic matter contains more aromatic linkages or is more crosslinked, so that the

Table 2. Summary of pyrolysis (pyrogram) data for Peru sediments and comparison to other areas.

Sample, interval (no. analyses)	Water depth (m)	P_1	P_2	T_{max} (°C)	TOC (%)	Correlation coefficients		
		(μg/g dry weight sediment)				P_2 vs. TOC	P_1 vs. TOC	P_1 vs. P_2
			. . . . Range	(average)				
ODP sediments								
681B, 0.4–3 m (24)	150	600–2,300	8,000–25,000	457–466	2–8	0.78	0.18	0.47
6–6.8 m (23)		50–850	7,000–23,000	455–470		nd	nd	nd
683A, 1.04–1.09 (22)	3000	200–700	5,500–8,000	462–472	0.8–1.5	0.22	0.003	0.5
686A, 19.35–20.4 (35)	450	100–500	3,400–6,100	447–461	2–5	0.5	0.001	
								0.11
Surface sediments								
SC4, 0–0.7 m (15)	92	50–520	1,000–11,000	455–463	1–4	0.9	0.83	
SC6, 0–0.55 m (13)	268	1000–3000	22,000–65,000	452–486	3.5–10	0.38	0.13	
MWSC7, 0–0.22 (19)	90	350–1100	9,000–20,000	450–462	2.7–4.1	0.58	0.31	0.92
SC12, 0–0.36 (11)	506	500–2000	12,000–60,000	446–457	2.5–10	0.95	0.84	
BC7, 0–0.24 (8)	85	20–500	350–11,000	433–464	1.5–4	0.23	0.24	
Non-Peru surface sediments								
Mississippi Fan-								
DSDP Leg 96 sites:								
623, 9–151 m (28	3,177		90–800 (500)	462–479	0.6–1.4	0	nd	
615, 14–504 m (20)	3,268		300–1,000	467–478	nd	nd	nd	
619, 0–167 m (10)	2,259		343–1,672 (750)	468 ± 3.5	0.65–1	0.28		
Walvis Ridge: DSDP	4,629	20–708	300–96,000	nd	0.6–17	0.90	0.52	
Leg 75, 940–1100 m								
Costa Rica Rift:	3,470	25–250	50–2,000		1–2.5	0.96		
DSDP Leg 69, Site								
504 10–236 m (28)								
505, 1–232 (18)	3,500	50–600	50–3,500		1–3.5	0.84		
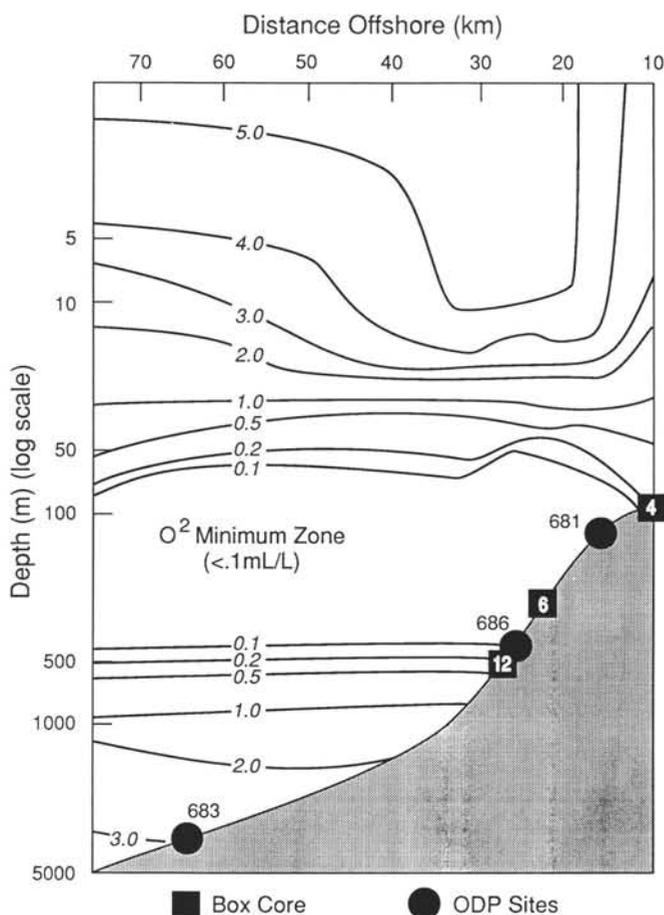
Figure 3. Diagram showing position of oxygen-minimum zone across Peru shelf and slope during Woods Hole 1978 cruise at 15°S.

resulting kerogen carbon-carbon bonds are harder to pyrolyze than those in the more marine (and more aliphatic) Peru organic material or (2) a greater proportion of recycled organic matter occurs in the Mississippi Fan sediments. A significant portion of the Mississippi Fan sediment organic material, even in immature sediments, was either eroded from continental sources and contained significant proportions of recycled and higher-land-plant material or represented organic matter rafted from shallow-water coastal environments that was exposed to intense biological reworking before the most recent burial within the fan (Whelan, 1986; Bouma, Coleman, et al., 1986).

For the ODP Peru sections analyzed here, the following trends in T_{max} values can be observed:

1. The T_{max} values for P_2 are in the range expected for immature surface sediments (446° to 472°C). For comparison, T_{max} values measured using the CDS instrument in our laboratory for more thermally mature sediments from the Alaskan North Slope typically range from 480° to 560°C for sediments containing only indigenous (rather than migrated) hydrocarbons and having vitrinite reflectance values ranging from $R_o =$ 0.4% to 0.8% (Whelan et al., 1986b). These R_o values are typical of thermal maturities just prior to and within the early part of the catagenetic petroleum generation range (maximum geothermal exposures in the range of 40° to 100°C).

2. Comparison of profiles of Peru ODP T_{max} values with those obtained for Peru Woods Hole surface (Table 1) and immature Mississippi Fan sediments (Whelan and Tarafa, 1986) suggests that the small- and short-scale changes in T_{max} profiles (such as those from 6.2 to 6.45 m in Hole 681B, Figure 6B; 19.35 to 19.6 m in Hole 686A, Fig. 8; and 2.6 to 2.78 m in Hole 683A, Fig. 11) represent oscillations in the relative influx of either reworked marine or terrigenous material (higher T_{max}) and more unaltered marine material (lower T_{max}). Support for the idea of higher T_{max} values being associated with more terrigenous or reworked organic matter comes from Table 2, which presents a comparison of values from a variety of immature surface with DSDP sediments containing varying proportions of terrigenous and marine organic matter. Thus,
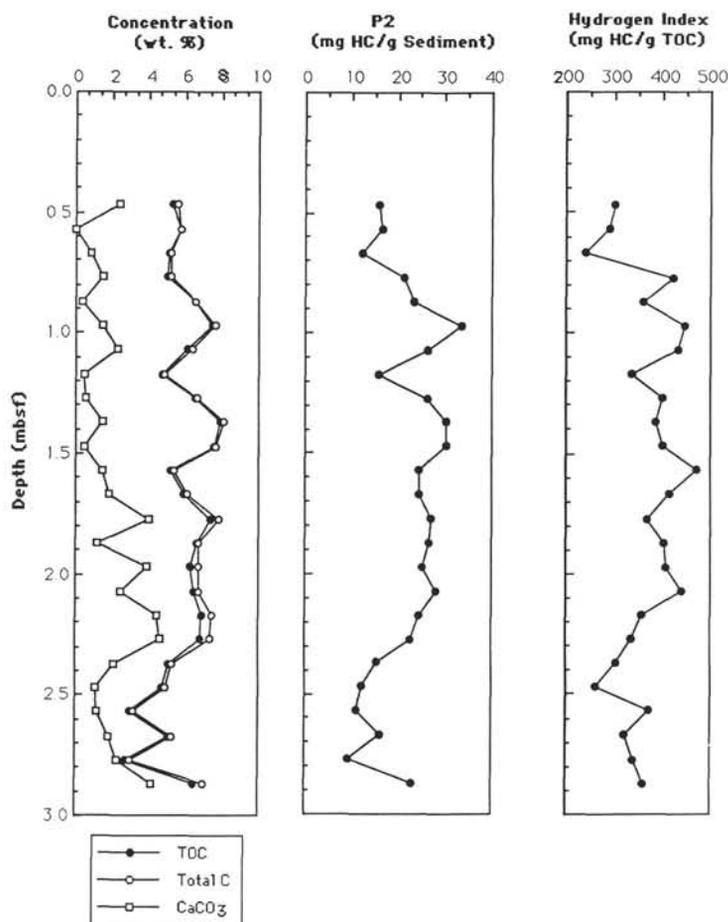
Figure 4. Summary of total carbon, TOC, P_2, and HI for surface section, Hole 681B, 0 to 3 mbsf. (Scale of $CaCO_3$ is 10× measured concentration.)

the DSDP Leg 96 Mississippi Fan sediments, which contain a high proportion of terrigenous organic matter (Jasper, 1988), have T_{max} values that are approximately 5° to 10°C higher than those for the Peru surface sediments.

Evidence for a contribution of traces of terrigenous organic matter to some sections of Woods Hole surface cores is provided by the presence of methoxy phenols as pyrolysis products, characteristic of high molecular-weight organic matter derived from lignin in higher plants from terrigenous sources, in a few sections, such as the 33 to 39 cm section of Core SC6 (Whelan et al., unpubl. data). Microscopic data support this hypothesis: the 33 to 39 cm section of Core SC6 also shows predominantly marine amorphous organic matter with some single algal, cuticle, and vitrinite particles (C. Thompson-Rizer, unpubl. data). We do not yet have the detailed PY-GCMS or microscopic data needed to determine if this is also the case for some of the Peru ODP sections examined here.

Farrington et al. (1988) proposed several possible scenarios for fluctuations in lipid biomarker profiles in the surface sediments at 15°S that may also apply to changes in T_{max}. These scenarios include (1) greater proportions of terrigenous material (i.e., higher T_{max}) that are caused by periods of increased El Niño activity, which result in decreased marine primary productivity and increased rainfall and terrigenous runoff; (2) changes in ocean currents, causing increased amounts of deposition and redeposition of inshore terrigenous sediments; (3) increased water depth, causing greater reworking in the water column before deposition, and/or (4) shifts in

the oxygen-minimum zone, causing changes in carbon preservation. Henrichs and Reeburgh (1987) reviewed the evidence and suggested that point (4) may be overrated as a cause of carbon preservation. These authors concluded from a review of recent microcosm and laboratory studies that anaerobic degradation is not intrinsically lower or slower than aerobic degradation and that fresh organic matter degrades at similar rates under oxic and anoxic conditions, assuming adequate electron acceptors are present in each case. However, if oxygen is not initially present, other electron acceptors (e.g., nitrate, sulfate, etc.) may be depleted more quickly so that more organic matter will be preserved. The decomposition rates of organic matter may also be slower in anoxic zones beneath the sediment/water interface when the most labile fraction of the organic matter has not survived to be buried. Reeburgh and Henrichs (1987) noted a possible modest slow-down of breakdown rates of anaerobic over aerobic organic matter, about two or three times in some cases, which would not be observable over geologic time. Furthermore, they also noted that increased activity of macrofauna in oxidizing sediments, rather than the presence of oxygen *per se*, accelerates the organic breakdown rates.

Total Carbon, Total Organic Carbon, and Hydrogen Indexes (P_2/TOC)

Pyrolysis P_2 data are shown along with total carbon, total TOC, and HI values in Figures 4, 6A, 7, and 10. The HI indicates the proportions of hydrogen-rich relative to hydrogen-poor organic carbon in the sediments.
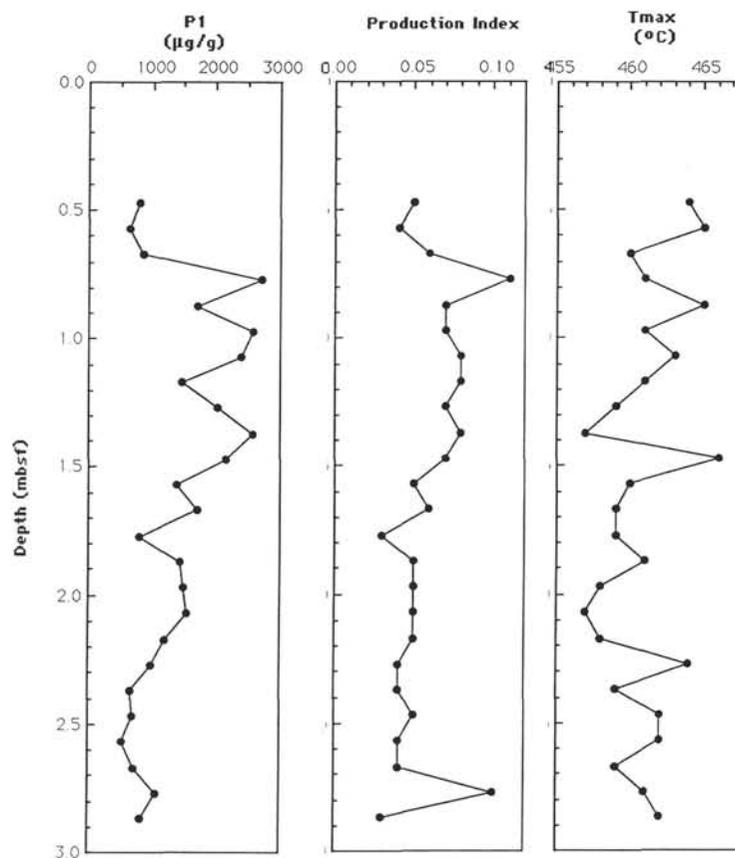
Figure 5. P_1, PI, and T_{max} pyrolysis data for Hole 681B, surface, 0 to 3.0 mbsf.

The 0.5 to 3 m section of Hole 681B has little carbonate carbon (Fig. 4) (consistent with a high influx of siliceous material and its position within today's upwelling zone), so that TOC and total carbon profiles might almost be superimposed. This section shows a good correlation between the P_2 and TOC ($r = 0.78$, Table 2). However, even with a good correlation, Figure 4 indicates that the two parameters exhibit distinct differences so that one can see maxima and minima in HIs. For example, two intervals where the HI reaches a minimum of about 240 mg hydrocarbon per gram of organic carbon occur at 0.65 and 2.4 m; in the remainder of the 0 to 3m interval, this value fluctuates between 350 and 500 mg/g. These minima represent carbon that is more hydrogen-poor because of the presence of either more terrigenous or more reworked organic carbon in the two layers. Note that the minima cannot be seen in the organic carbon profile, where values remain relatively constant.

For comparison, similar data are shown in Figure 12 for much more closely spaced intervals from Woods Hole surface Core MWSC7. In this case, TOC is almost constant from 0 to 12.5 cm, while significant variations in P_1, P_2 (not shown), and HI can be seen. All three of these parameters decrease rapidly with depth over the top 4 cm, probably reflecting rapid biological reworking of the sediment within the surface sediment layer. The P_2 and TOC minimum in the bottom 16 to 20 cm section corresponds roughly to the interval where an increase in terrigenous and a decrease in marine lipid biomarkers occur in Core SC4, which comes from the same area and water depth (Table 2 and Farrington et al., 1988). This observation is consistent with the interpretation that one cause of decreasing P_1, P_2, and PI may be an increase in the proportion of terrigenous organic matter.

Total carbon, TOC, P_2, and HI data for the 19.3 to 20.4 mbsf section of Hole 686A are shown in Figure 7. A significantly higher contribution of carbonate carbon and lower amount of TOC (3% to 5% and 1.5% to 2%, respectively) is obvious at Site 686 when these values are compared with values from the Hole 681 core described above (0% to 0.5% and 3% to 8%, respectively). In the case of the 19.35 to 19.55 mbsf section from Hole 686A, there is considerably more variation in P_2 and the HIs than in either TOC or total carbon. Some maxima and minima in both P_2 and the HIs are evident in Figure 7, with some strong (possibly cyclic?) variation.

Some of the apparent cyclicity observed for P_1 in the 2.63 to 2.75 mbsf section of Hole 683A (Fig. 11) may also be present in HI, P_2, and TOC in the same section. As noted for the P_1 variations, there seems to be no correlation of maxima and minima in either P_2 or HI values with visual characteristics of the cores (Table 1). We previously noted that T_{max} values are generally higher for Hole 683A than for either of the other two holes (Table 2). The T_{max} values also exhibit strong oscillation in the same parts of the hole, where the cyclicity in P_1, P_2, and HI can be seen (Figs. 10 and 11). Our tentative hypothesis for these oscillations in P_2, HI, and T_{max} values for Hole 683A is that the samples from Site 683 received periodic influxes of refractory reworked (resuspended) or terrigenous clastic material, causing a slight increase in T_{max} and a decrease in P_2 (and, in some instances, depending upon changes in carbon sources within particular intervals, oscillations in the HIs). The geology and sedimentology of lithologic Unit I of Site 683 is most consistent with periodic influxes of more refractory organic matter derived from redeposition of upslope sediments caused by changes in sea level, tectonic rearrangement of the shelf, or changes in the proportions of
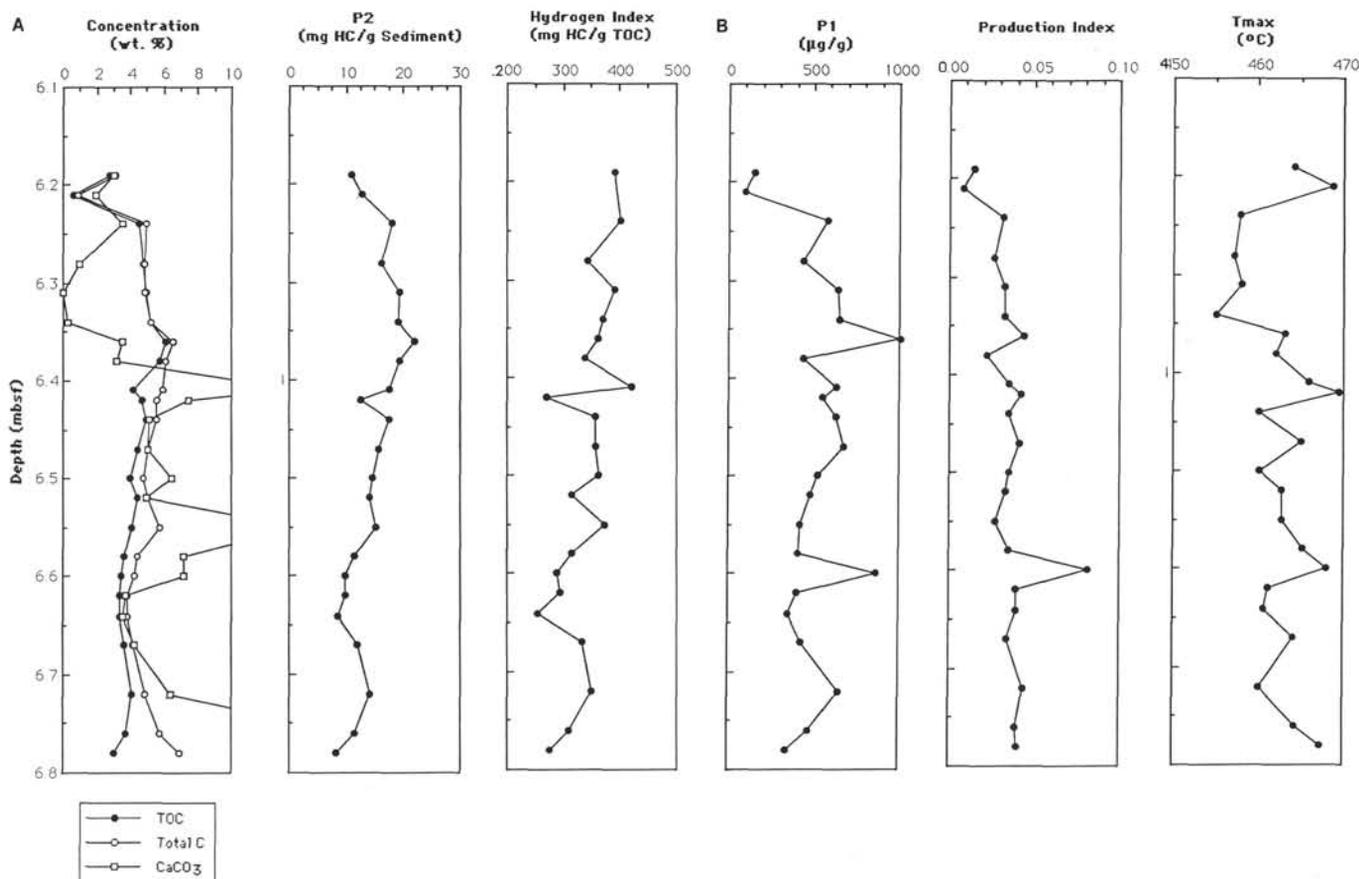
Figure 6. A. Summary of pyrolysis data, Hole 681B, 6.2 to 6.8 mbsf, total carbon, TOC, P_2, and HI. B. Summary pyrolysis data, Hole 681B, 6.2 to 6.8 mbsf, P_1, PI, and T_{max}. (Scale of $CaCO_3$ is 10× measured concentration.)

terrigenous clastic influx and marine biogenic organic matter produced in the upwelling zone (Suess, von Huene, et al., 1988). The more refractory nature of organic matter in some sections may be due to resuspension of shelf sediment, followed by redeposition downslope and dilution of fresh marine material. Using DSDP Leg 95 sediments from offshore New Jersey, Tarafa et al. (1987) found that slumped sediments tended to have higher HI and lower T_{max} values than non-slumped sediments that were deposited more slowly. Some of the same influences may have operated at this site. Turbidite interbeds occur in Unit I, but locations are hard to pinpoint. There are layers having graded bedding at about 2.2 to 2.7 mbsf and numerous small layers with terrigenous materials (i.e., silts and clays) throughout the section.

Variations in proportions of influx of terrigenous to marine sediments may also explain oscillations in P_2, HI, and T_{max} values in the Site 686 sediments described above. Site 686 had a pronounced terrigenous influx throughout the entire section. However, this terrigenous material may be more pronounced for Site 683. This view is consistent with T_{max} values at Site 686A that are slightly lower than those of Site 683 sediments (Table 2). Site 683 sediments may thus contain a higher contribution of more reworked or more terrigenous organic matter. However, the differences may also be related to water depth: Site 683 is located at a water depth of 3071 m, while Site 686 is at 307 m. The greater depth at Site 683 allowed for greater reworking of organic matter in the water column prior to sediment deposition.

Table 2 presents a comparison of P_2, TOC values, and correlations of the two parameters in Peru surface and ODP

sediments; organic-rich Walvis Ridge sediments (interbedded black, gray, and green Cretaceous shales, DSDP Leg 75, water depth 3000 m, Jasper et al., 1984); open-ocean Costa Rica Rift sediments (DSDP Sites 504 and 505; water depth 2500 m, Whelan and Hunt, 1982); and the terrigenous Mississippi Fan sediments discussed previously (DSDP Leg 96 sediments, Whelan, 1986; Whelan and Tarafa, 1986). The Walvis Ridge P_2 and organic carbon values exhibit the widest ranges, but also exhibit very good correlation ($r = 0.9$). The P_2 values for the marine Costa Rica Rift sediments from Sites 504 and 505 also show good correlations with TOC ($r = 0.96$ and 0.84, respectively). However, the correlation of TOC with P_2 is poor for DSDP Site 619 from the Gulf of Mexico ($r = 0.28$), which contains significant contributions of both terrigenous and marine organic matter (Jasper 1988). This comparison suggests that a good correlation of P_2 with TOC may be indicative of a consistent influx source (e.g., predominantly marine, as for the Walvis Ridge and Costa Rica Rift sediments). In the case of the Peru ODP sediments, the higher correlation of P_2 with TOC for Hole 681B sediments ($r = 0.78$) than for the Holes 683A or 686A sediments ($r = 0.22$ and 0.3, respectively, Table 1) is consistent with a higher influx of marine organic matter to Hole 681B than to either of the other two sites. It is interesting that Hole 683A, which gives the poorest correlation, is also the site that we suspect is most strongly influenced by reworked and terrigenous organic matter.

However, data from the Woods Hole surface sediments suggest that the reasons for correlation or lack thereof between P_2 and HI are considerably more complex than sug-
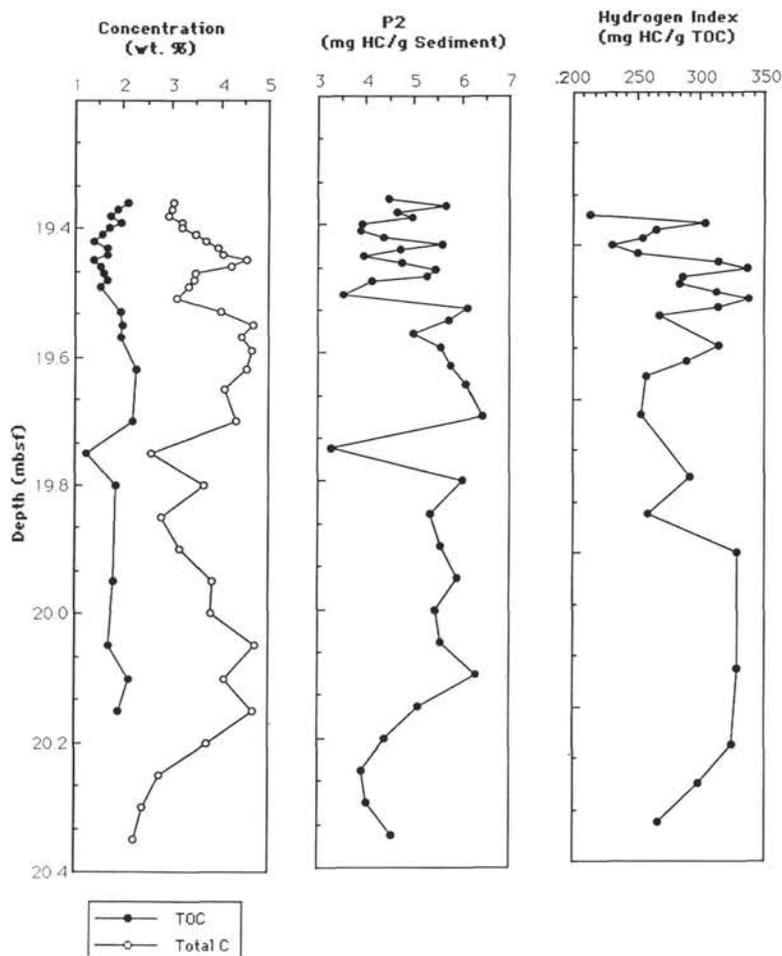
Figure 7. Summary of total carbon, TOC, P_2, and HI data, Hole 686A, 19.35 to 19.60 mbsf.

gested above. Poor correlations were observed for Cores BC7 ($r = 0.23$) and MWSC7 ($r = 0.44$), both of which are located on the shelf at the edge of the oxygen-minimum zone and might contain significant proportions of reworked, as well as traces of, terrigenous organic matter. However, an excellent correlation was observed for Cores SC4 ($r = 0.9$) from the same region. Core SC12, recovered from the oxygen-minimum zone of the upwelling region, contains predominantly marine organic matter and gives an excellent correlation ($r = 0.95$). However, Core SC6 from the same region does not show a good correlation ($r = 0.38$), which is consistent with the pyrolysis GCMS data that suggest the presence of some contribution of reworked or terrigenous organic matter in deeper sections of this core. These data suggest that both a consistent organic source (i.e., marine or terrigenous) and a consistent degree of reworking are necessary to produce a good correlation of P_2 with TOC.

Pyrolysis-Gas Chromatography Mass Spectrometry

To date, one sample from each ODP Peru site has been analyzed in detail to compare ODP sediment PY-GCMS patterns with more detailed data already obtained for the Woods Hole Peru surface samples. In Table 4, a qualitative summary of the types of pyrolysis products found in ODP samples (determined by GCMS) is given; this is then compared to typical patterns found for surface sediments that contain well-characterized sources of organic matter. These Leg 112 results are preliminary, and additional analyses need

to be run, specifically to look in detail at some of the Site 683 sections, where the presence of more terrigenous material has been suggested by the pyrogram data discussed above.

PY-GCMS data for the Leg 112 samples are similar to those obtained for more detailed samples from Woods Hole surface cores, as summarized in Table 4. Most of the Peru samples show strong a pyrolysis signal for pyrroles that can be derived either from porphyrins or chlorins (such as chlorophyll), amino sugars (including chitins), or proteins (van de Meent, 1980; Sigleo et al. 1982; Lal and Hayes, 1985). This pyrrole pyrolysis signal is uniformly strong in most of the Peru surface and ODP sediments examined to date. Pyrrole pyrolysis products are either weaker or missing in surface or immature sediments that contain a larger fraction of terrigenous material, including sediments from the Cape Lookout Bight area off the North Carolina coast, on which considerable research was performed by Martens and co-workers (Haddad and Martens, 1987), a Georgia estuary sediment (Whelan et al., 1986a), and DSDP Mississippi Fan sediments from Leg 96 (Whelan and Tarafa, 1986). Out of a total of 15 Peru surface sediment sections examined to date, we found that the pyrrole pyrolysis signal was weak in only one (Core SC6, 33–39 cm). Although this particular sample comes from the center of the upwelling area, all of the lipid biomarker and pyrolysis data examined to date consistently show a larger contribution of terrigenous material to this specific interval, as summarized below.

Methoxyphenol pyrolysis products are derived from lignin, which can come only from the woody sections of terrigenous
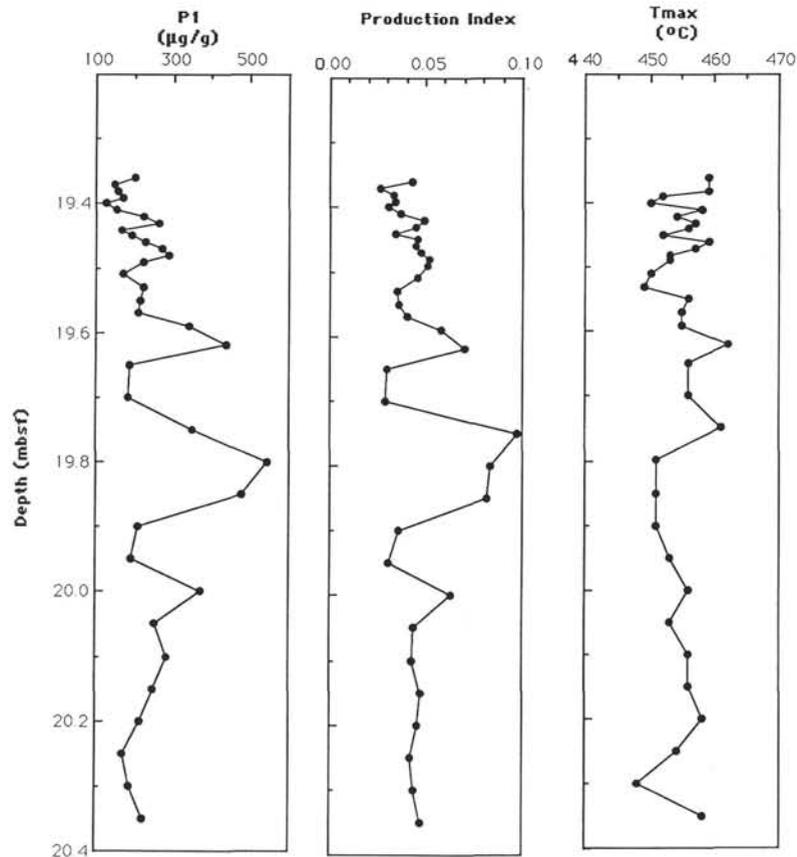
Figure 8. Summary of pyrolysis data, Hole 686A, 19.35 to 19.60 mbsf, P_1, PI, and T_{max}.

higher plants (Martin et al., 1979; Saiz-Jimenez and de Leeuw, 1984, 1985; van de Meent et al., 1980; Sigleo et al., 1982; Bracewell et al., 1980; Whelan et al., 1986a and references cited therein). These products are absent in all of the Woods Hole Peru surface cores, with the exception of Core SC6 intervals (33–39cm) and a possible trace in the nearshore Core BC7 (12–16cm), a fact consistent with very little influx of terrigenous organic matter. Recent C_{37} alkenone data (Farrington et al., 1988) show that higher sea-surface temperatures prevailed during deposition of the 33 to 39 cm section of Core SC6 than during deposition of shallower sections, an observation consistent with deposition of this 33 to 39 cm section during a period of strong El Niño activity; El Niño events typically decrease marine primary productivity and increase sea-surface temperatures and rainfall along the Peru coast (Barber and Chavez, 1983; Quinn et al., 1987). Increased continental runoff, therefore, may have caused an increased influx of the sparse terrigenous organic matter from the desertlike coast into the 33 to 39 cm section of Core SC6. Core BC7 (12–16 cm) was recovered nearer the shore and exhibits evidence of terrigenous influx in the lipid extracts (Volkman et al., 1983). In contrast to the Peru cores, the methoxy phenol pyrolysis products are prominent in the Cape Lookout Bight and Georgia Estuary cores, which contain significant amounts of terrigenous material. Methoxyphenols could not be detected in the DSDP Mississippi Fan cores, which also contain significant quantities of terrigenous organic matter (Whelan, 1986). However, Hedges et al. (1985) presented evidence that lignins, from which the methoxyphenols are derived, often do not survive in deeper sediments.

The homologous n-alkane/1-alkene doublets are characteristic pyrolysis products of some lipid materials (e.g., van de Meent et al., 1980; Seiglio et al., 1982; Larter, 1984; Irwin, 1982). In other research, we found that these homologous doublets extend up to fairly high carbon numbers (at least to C_{28}) in samples containing significant amounts of lipid-rich, terrigenous organic matter (derived largely from higher plant waxes), such as the Messel Shale from Europe, the Green River shale from the U.S., and sediments from Georgia and Cape Lookout Bight (data summarized in Table 4). These doublets are either missing or weak in the Peru samples, including those from the ODP sites, with the exception of Core SC6 (33–39 cm) discussed previously and a few others where the signal is much weaker.

Aromatic pyrolysis products also were examined. These were strong in all of the samples in Table 4 and exhibited no obvious qualitative differences between the Peru and the other more terrigenous samples, except that these products seemed to be a little stronger in the more terrigenous samples. Heterocyclic sulfur pyrolysis products (primarily alkyl thiophenes) are distributed sporadically in Peru sediments, and sometimes in sediments from other geographic areas. Research is in progress to learn more about the precursors of these pyrolysis products. One possible precursor in the Peru sediments may be the *Thioploca* bacterial mats that have been observed to be associated with low-oxygen bottom waters in the region (Gallardo, 1977; Rosenburg et al., 1983; Henrichs and Farrington, 1984; and McCaffrey et al., 1989). Thus, pyrolysis of a strand of *Thioploca* was performed to give the results shown in Table 4. The *Thioploca* showed a series of

Figure 9. Close-up photograph showing laminated sediment from interval 112-686A-3H-4, 50–69 cm (19.38–19.57 mbsf).

SUMMARY AND CONCLUSIONS

1. Pyrolysis of closely spaced samples from surface sediments from Site 681 generally showed higher amounts of pyrolyzable carbon than samples from either Site 683 or Site 686, which is consistent with the shallow-water position of Site 681 within the upwelling zone. A cyclical pattern of P_1, P_2, and PI values may be present in the shallowest sections examined from both Sites 683 and 686, corresponding to a roughly 500 yr or less periodicity. Evidence of these cycles could be seen at Site 686, but not at Site 683. In the case of Site 686, higher P_1 and P_2 values generally corresponded to more laminated sections.

2. T_{max} values were consistently higher for the Site 683 samples than for those from the other two sites, possibly reflecting a greater influx of more reworked or pre-altered and possibly some terrigenous material to this site, which is situated downslope of the upwelling zone in deep water.

3. P_1 and PI values for all three sections are consistent with P_1 constituents inherited directly from the biologically derived organic matter in the sediment, rather than coming from the thermal decomposition of kerogen (i.e., petroleum catagenesis).

4. PY-GCMS patterns for one sample from each ODP site was compared with Peru surface samples (from Woods Hole cruises) and with surface and immature sediments having a more terrigenous influx. Results are consistent with the three ODP samples examined so far being strongly influenced by marine upwelling with little or no terrigenous influx.

5. *Thioploca* bacterial mats, diagnostic of low-oxygen (<0.1 mL/L) bottom waters, are one possible source of the sporadic thiophene pyrolysis products observed in some Peru sediments.

REFERENCES

Arnosti, C., and Müller, P. J., 1987. Pyrolysis-GC characterization of whole rock and kerogen-concentrate samples of immature Jurassic source rocks for N.W. Germany. *Org. Geochem.*, 11:505–512.

Barber, R. T., and Chavez, F. P., 1983. Biological consequences of El Niño. *Science*, 222:1203–1210.

Bracewell, J. M., Robertson, G. W., and Welch, D. I., 1980. Polycarboxylic acids as the origin of some pyrolysis products characteristic of soil organic matter. *J. Anal. Appl. Pyrol.*, 2:239–248.

Bouma, A. H., Coleman, J. M., et al., 1986. *Init. Repts. DSDP*, 96: Washington (U.S. Govt. Printing Office), 1–247.

Curry, W. B., and Miller, K. G., in press. Oxygen and carbon isotopic variation in Pliocene benthic Foraminifers of the Equatorial Atlantic. *Proc. ODP, Sci. Results*, 108: College Station, TX (Ocean Drilling Program).

Durand, B., and Monin, J. C., 1980. Elemental analysis of kerogens (C, H, O, N, S, and Fe). *In* Durand, B. (Ed.), *Kerogen*: Paris (Editions Technip), 113–142.

Espitalié, J., Marquis, F., and Barsony, I., 1984. Geochemical logging. *In* Voorhees, K. J. (Ed.), *Analytical Pyrolysis:* London (Butterworths), 276–304.

Farrington, J. W., Davis, A. C., Sulanowski, J., McCaffrey, M. A., McCarthy, M., Clifford, C. H., Dickinson, P., and Volkman, J. K., 1988. Biogeochemistry of lipids in surface sediments of the Peru upwelling area at 15°S. *Organic Geochem.*, 13:607–617.

alkyl thiophenes as major pyrolysis products (in comparison to other samples described in Table 4). The exact mechanism by which these arise must await further research. However, our results do suggest that one possible source of these thiophenic pyrolysis products in other sediments might be thermal reactions of *Thioploca*, although other potential sources are also possible in sulfur-rich anoxic marine sediments.

Gallardo, V. A, 1977. Large benthic microbial communities in sulphide biota under Peru-Chile subsurface countercurrent. *Nature*, 268:331–332.

Haddad, R., and Martens, C., 1987. Biogeochemical cycling in an organic-rich coastal marine basin—9. Sources and accumulation rates of vascular plant-derived organic material. *Geochem. Cosmochim. Acta*, 51:2991–3002.

Hedges, J. I., Cowie, G. L., Ertel, J. R., Barbour, R. J., and Hatche, P. G., 1985. Degradation of carbohydrates and lignins in buried woods. *Geochim. Cosmochim Acta*, 79:701–711.

Henrichs, S. M., and Farrington, J. W., 1984. Peru upwelling region sediments near 15°S—l. Remineralization and accumulation of organic matter. *Limnol. Oceanogr.*, 29:1–19.

Henrichs, S. M., Farrington, J. W., and Lee, C., 1984. Peru upwelling region sediments near 15°S—II. Dissolved free and total hydrolyzable amino acids. *Limnol. Oceanogr.*, 29:30–34.

Henrichs, R. M., and Reeburgh, W., 1987. Anaerobic mineralization of marine sediment organic matter: rates and role of anaerobic processes in the oceanic carbon economy. *Geomicrobiol. J.*, 5:191–237.

Horshfield, B., 1984. Pyrolysis studies and petroleum exploration. *In* Brooks, J., and Welte, D. (Eds.), *Advances in Petroleum Geochemistry*: New York (Academic Press), 247–298.

Irwin, W. J., 1982. *Analytical Pyrolysis, A Comprehensive Guide*. Chromatographic Science Series, 22: New York (Dekker), Chapter 7.

Jasper, J. P., 1988. *An Organic Geochemical Approach to Problems in Glacial Interglacial Climate Variability*. [PhD thesis]. Massachusetts Institute of Technology/Woods Hole Oceanographic Institution Joint Program in Chemical Oceanography, Woods Hole Oceanographic Institution, Woods Hole, MA.

Jasper, J. P., Whelan, J. K., and Hunt, J. M., 1984. Migration of C1–C8 volatile organic compounds in sediments from the Deep Sea Drilling Project, Leg 75, Hole 530A. *In* Hay, W. W., Sibuet, J. C., et al, *Init. Repts. DSDP*, 75: Washington (U.S. Govt. Printing Office), 1001–1008.

Katz, B. J., 1983. Limitations of "Rock-Eval" pyrolysis for typing organic matter. *Org. Geochem.*, 4:195–199.

Lal, G. S., and Hayes, E. R., 1985. Determination of amine content of chitosan by pyrolysis gas chromatograph. *J. Anal. Appl. Pry.*,

Larter, S. R., 1984. Application of analytical pyrolysis techniques to kerogen characterization and fossil fuel exploration/exploitation. *In* Voorhees, K. J. (Ed.), *Analytical Pyrolysis*: London (Butterworths), 212–275.

Martin, F., Saiz-Jimenez, C., and Gonzalez-Vila, F. J., 1979. Pyrolysis-gas chromatograph—mass spectrometry of lignins. *Holzforschung*, 33:210–212.

McCaffrey, M. A., Farrington, J. W., and Repeta, D., 1989. Geochemical implications of the lipid composition of *Thioploca* from the Peru upwelling region—15°S. *Org. Geochem.*, 14:61–68.

Martens, C. S., and Klump, J. V., 1984. Biogeochemical cycling in an organic rich coastal marine basin—4. An organic carbon budget for sediments dominated by sulfate reduction and methanogenesis. *Geochim. Cosmochim. Acta*, 48:1987–2004.

Orr, W. L., 1981. Comments on pyrolytic hydrocarbon yields in source-rock evaluation. *In* Bjoroy, M. (Ed.), *Advances in Organic Geochemistry 1981*: New York (Wiley), 775–782.

Peters, K. E., 1986. Guidelines for evaluating petroleum source rocks using programmed pyrolysis. *AAPG Bull.*, 70:318–329.

Philp, P., 1985. *Fossil Fuel Biomarkers, Applications and Spectra*: New York (Elsevier), 1–294.

Ouinn, W. H., Neal, V. T., and Antunez de Mayolo, S. E., 1987. El Niño occurrences over the past four and a half centuries. *J. Geophys. Res.*, 92:14449–14461.

Rosenberg, R., Arntz, W. E., de Flores, E. C., Flores, L. A., Carbajal, G., Finger, I., and Tarazona, J., 1983. Benthos biomass and oxygen deficiency in the upwelling system off Peru. *J. Mar. Res.*, 41:263–279.

Saiz-Jimenez, C., and de Leeuw, J. W., 1985. Chemical characterization of soil organic matter fractions by analytical pyrolysis-gas chromatography-mass spectrometry. *J. Anal. Appl. Pry.*, 9:99–119.

Saiz-Jimenez, C., and de Leeuw, J. W., 1984. Pyrolysis-gas chromatography-mass spectrometry of isolated, synthetic and degraded lignins. *Org. Geochem.*, 6:417–422.

Sigleo, A. C., Hoering, T. C., and Helz, G. R., 1982. Composition of estuarine colloidal material: organic components. *Geochim. Cosmochim. Acta*, 46:1619–1629.

Suess, E. von Huene, R., et al., 1988. *Proc. ODP, Init. Repts.*, 112: College Station, TX (Ocean Drilling Program).

Tarafa, M. E., Whelan, J. K., and Mountain, G. S., 1987. Sediment slumps in the middle and lower Eocene of DSDP Holes 605 and 613: chemical detection by pyrolysis techniques. *In* Poag, C. W., Watts, A. B., et al., *Init. Repts. DSDP*, 95: Washington (U.S. Govt. Printing Office), 661–669.

Tissot, B. P., 1984. Recent advances in petroleum geochemistry applied to hydrocarbon exploration, *AAPG Bull.*, 68:545–563.

Tissot, B. P., and Welte, D., 1984. *Petroleum Formation and Occurrence*: New York-Berlin-Heidelberg (Springer-Verlag), 1–699.

Shipboard Scientific Party, 1980. Drilling Project Site 436. *In* Honza, et al., *Init. Repts. DSDP*, 56,57: Washington (U.S. Govt. Printing Office), 921–935.

Ungerer, P., Espitalié, J., Marquis, F., and Durand, B., 1986. Use of kinetic models of organic matter evolution for the reconstruction of paleotemperatures. Application to the case of the Gironville Well (France). *In* Burrus, J. (Ed.), *Thermal Modeling in Sedimentary Basins*: Paris (Editions Technip), 531–546.

Van de Meent, D., de Leeuw, J. W., and Schenck, P. A., 1980. Chemical characterization of non-volatile organics in suspended matter and sediments of the River Rhine Delta. *J. Anal. Appl. Pry.*, 2:249–263.

Volkman, J. K., Farrington, J. W., Gagosian, R. B., and Wakeham, S. G., 1983. Lipid composition of coastal marine sediments from the Peru upwelling region. *In* Bjorøy, M. (Ed.), *Advances in Organic Geochemistry, 1981*: New York (Wiley), 228–240.

————, 1987. Marine and terrigenous lipids in coastal sediments from the Peru upwelling region at 15°S: sterols and triterpene alcohols. *Org. Geochem.*, 11:463–477.

Whelan, J. K., 1986. Geochemistry summary—Leg 96—the Mississippi Fan. *In* Bouma, A., Coleman, J., et al., *Init. Repts. DSDP*, 96: Washington (U.S. Govt. Printing Office), 691–695.

Whelan, J. K., and Hunt, J. M., 1982. Organic matter in Deep Sea Drilling Project Sites 504 and 505 sediments studied by a thermal analysis-gas chromatography technique. *In* Cann, J. R., Langseth, M. G., et al., *Init. Repts. DSDP*, 69: Washington (U.S. Govt. Printing Office), 443–450.

————, 1983. Volatile C1–C8 organic compounds in sediments from the Peru upwelling region. *Org. Geochem.*, 5:13–28.

Whelan, J. K., Farrington, J. W., and Tarafa, M. E., 1986a. Maturity of organic matter and migration of hydrocarbons in two Alaskan North Slope wells. *Org. Geochem.*, 10:207–219.

Whelan, J. K., Fitzgerald, M., and Tarafa, M.E., 1983. Analyses of organic particulates from Boston Harbor by thermal distillation-pyrolysis. *Environ. Sci. Tech.*, 17:292–298.

Whelan, J. K., Hunt, J. M., and Huc, A. Y., 1980. Applications of thermal distillation-pyrolysis to petroleum source rock studies and marine pollution. *J. Anal. Appl. Pyrol.*, 2:79–96.

Whelan, J. K., and Tarafa, M., 1986. Organic matter in Leg 96 sediments—characterization by pyrolysis. *In* Bouma, A., Coleman, J., et al., *Init. Repts. DSDP*, 96: Washington (U.S. Govt. Printing Office), 757–766.

Whelan, J. K., Tarafa, M. E., and Sherr, E. B., 1986b. Phenolic and lignin pyrolysis products of plants, seston, and sediment in a Georgia estuary. *In* Sohn, M. (Ed.), *Organic Marine Geochemistry Advances in Chemistry, Series No. 305*: Washington (Am. Chem. Soc.), 62–75.
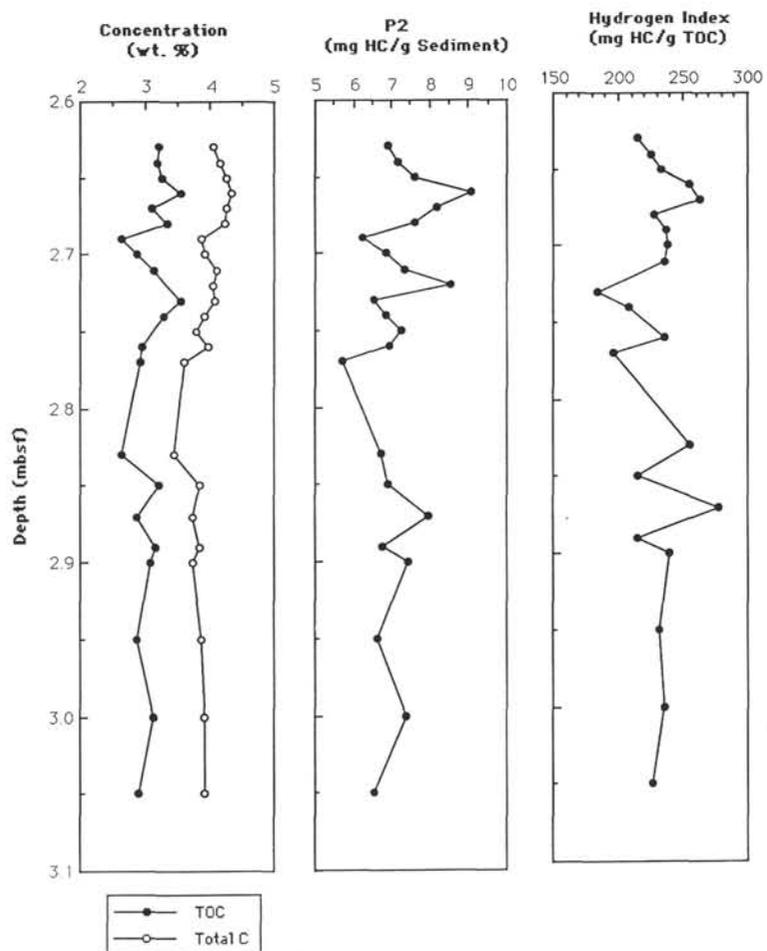
Figure 10. Summary of total carbon, TOC, P₂, and HI, Hole 683A, 2.6 to 3.1 mbsf.
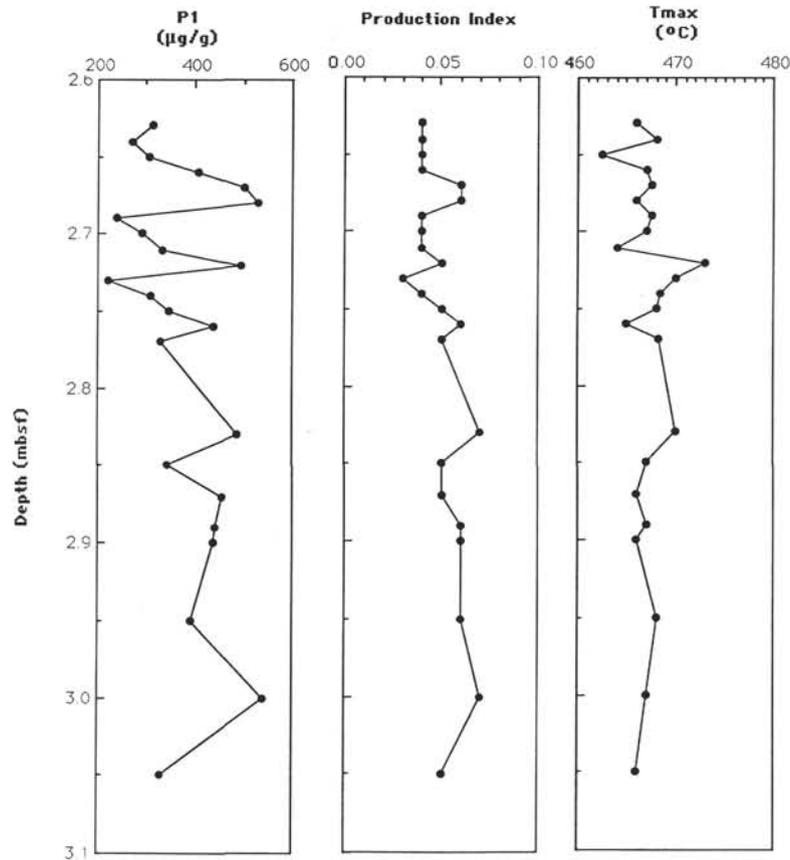
Figure 11. Summary of pyrolysis data, Hole 683A, 2.6 to 3.1 mbsf, P_1, PI, and T_{max}.

Table 3. Comparison of CDS (Woods Hole) with Rock-Eval (shipboard) data.

	Woods Hole (CDS) data				Rock—Eval (shipboard) data			
Sample (no. analyses)	P_1	P_2	T_{max} (°C)	TOC (%) (WHOI)	S_1	S_2	T_{max}, (°C)	TOC (%)
	(μg/g dry weight)				(μg/g dry weight) Range			
81B, 0.4–3 m (24)	600–2,000	8,000–25,000	457–466	2–8	1,430	6,600	400 [a](460)	1.87
6–6.8 m (23)	50–850	7,000–23,000	455–470		3,030	15,930	393 [a](453)	3.97
683A, 1.04–1.09m (22)	200–700	5,500–8,800	462–472	0.8–1.5	1,200	8,000	421 [a](481)	3
686A, 19.35–20.4 (35)	100–500	3,400–6,100	447–461	2–5	470–2,500	2,000–19,000	393–401 [a](453–461)	0.5–4.8

[a] Rock-Eval temperatures plus 60°C—correction required to calculate actual temperatures for comparison to CDS data—see "Methods" section (this chapter).

589
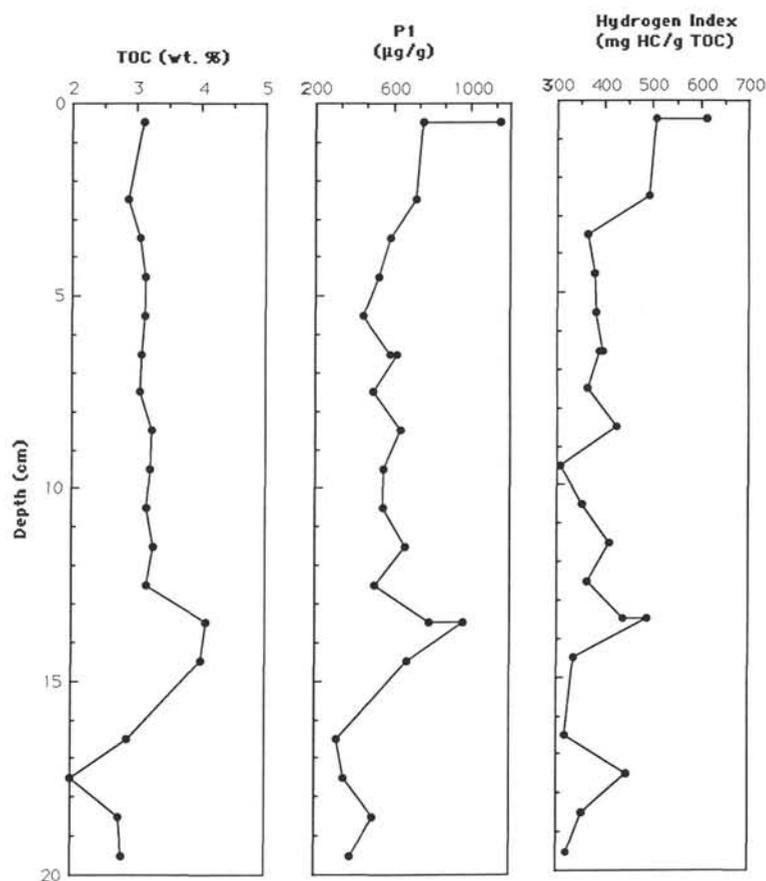
Figure 12. Summary of pyrolysis data, TOC, P_1, and HI for Woods Hole Peru surface Core MWSC7.

Table 4. Summary of pyrolysis GCMS characteristics, Leg 112 samples and comparison of surface and immature sediments from Peru with other areas having stronger terrigenous influx (Cape Lookout Bight, Georgia; Georgia Estuary; and Mississippi Fan DSDP sediments).

Sample Peru—Surface	N compounds (pyrroles)	Methoxyphenol (lignins)	Homologous n-alkene/l-alkenes	Aromatics	Sulfur compounds
(4 cores—upwelling region)	Strong	No (phenols only)	Weak	Some present	Variable
Peru—ODP—Sites 681, 683 & 686	Strong	No (phenols only)	Weak	Some present	Variable
Peru—Thioploca Bacteria	Strong (pyridines & indoles also)	No (but strong phenol signal)	No	Strong	Strong—several thiophenes present
Samples with some terrigenous flux:					
Cape Lookout Bight (1)	Little or none	Moderate	Strong signal to fairly high carbon number	Strong	Not determined
Georgia Estuary (2)	Litte or none	Very strong	Strong	Strong	Weak
Mississippi Fan (3)	Little or none	Traces	Strong	Strong	Moderate

(1) Whelan and Haddad, unpublished data as summarized in Haddad, Ph.D. Thesis, 1987.
(2) Whelan et al., 1986a.
(3) Whelan et al., 1986b.